

Flywheel Energy Storage for Ancillary Services: A Novel Design and Simulation of a Continuous Frequency Response Service for Energy Limited Assets

ANDREW J. HUTCHINSON^{ORCID} (Member, IEEE),
AND DANIEL T. GLADWIN^{ORCID} (Senior Member, IEEE)

Department of Electronic and Electrical Engineering, The University of Sheffield, S1 3JD Sheffield, U.K.

CORRESPONDING AUTHOR: A. J. HUTCHINSON (andrew.hutchinson@sheffield.ac.uk)

This work was supported by the Engineering and Physical Sciences Research Council (EPSRC) in the form of the "Energy Storage Integration for a Net Zero Grid" under Project EP/W02764X/1.

ABSTRACT With National Grid ESO introducing a suite of new Frequency Response Services for the GB electricity market, there is an opportunity to investigate the ability of low-energy capacity storage systems to participate in the frequency response market. In this study, the effects of varying the response envelope of the frequency response service on the performance of a standalone Flywheel Energy Storage System is assessed. In doing so, a new Frequency Response Service that would allow flywheels and other high-power, low-energy storage devices to participate in the frequency response market as standalone systems is designed. This results in a 20C FESS achieving a 95% availability over the course of a year of operation, representing an excellent level of performance under existing market conditions. This work shows that a far wider range of energy storage mediums have the capability to provide meaningful contributions to grid frequency control than was previously assumed. It is also shown for the first time that through tailoring a service to the advantages of a flywheel, significant economic benefits can be achieved, culminating in showing that a 20C FESS could provide a positive economic performance up to a total capital cost of £3,364/kW under current market conditions.

INDEX TERMS Flywheels, energy storage, frequency response, economic.

I. INTRODUCTION

DUE to the intermittent nature of most renewable energy, the balance between demand and generation is becoming more difficult to manage. Many countries offer contracts for energy storage installations to participate in where they will either charge or discharge in relation to frequency deviations. In Great Britain, multiple frequency response services have been introduced to help keep the grid frequency within operational limits by National Grid ESO (NGESO) who operate the GB electricity grid.

The extensive publicly available data for the previously operational Dynamic Frequency Response (DFR) service can provide an excellent basis to perform suitability assessments on the ability of energy storage to provide these services [1]. There has been wide-ranging research conducted using DFR as a benchmark, mainly using Battery Energy Storage

Systems (BESSs) [2] but less commonly exploring different technologies or distributed resources [3], [4], [5].

To replace DFR, NGESO have introduced a suite of three new frequency response services, namely Dynamic Containment (DC), Dynamic Regulation (DR) and Dynamic Moderation (DM) [6]. These three services are being introduced with different approaches to the objective of stabilising the frequency at 50Hz. Fig. 1 shows the response envelope of the services being discussed in this paper. These services have often been referred to as having been developed with a view of allowing a wider range of technologies to operate in the frequency response service market. Some research has suggested that this is not the case for low energy assets [7], [8], and therefore an opportunity exists to determine exactly what manner of service would be required for lower energy assets to compete in this industry.

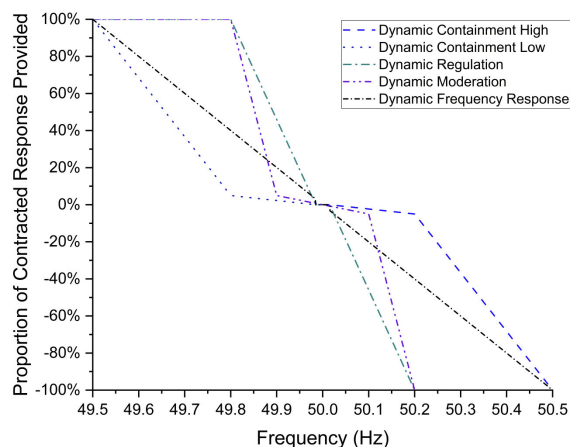


FIGURE 1. Response envelope for dynamic containment high and low, dynamic moderation, dynamic regulation and dynamic frequency response.

In many electricity markets worldwide, frequency regulation is referred to in terms of primary, secondary and tertiary regulation [9]. Primary regulation acts immediately after a frequency event, in the period of 0.2s-30s after a disturbance [10]. Secondary regulation then continues to operate from this point for several minutes after the disturbance, often quoted between 2 and 10 minutes. Tertiary regulation is then utilised in the aftermath of these services to ensure the frequency is maintained at its target value following the primary and secondary regulation [11].

It is important to note that the frequency response service discussed here does not align with these descriptors of frequency regulation. Where primary, secondary and tertiary regulation services are generally considered to operate post-fault, DFR and the new services DC, DM and DR, are all intended to be continuously provided regardless of network conditions to regulate the frequency of the grid under normal operational conditions due to regular fluctuations in load and demand. They are most similar to primary frequency regulation, reacting to the given frequency on a sub-second basis.

A. NOVEL CONTRIBUTION

This paper expands upon, develops, and presents new ideas and material on the previously presented conference paper [12]. In this journal, the bespoke profile previously presented is further developed, with a novel first-of-its-kind economic analysis presented on the potential for this bespoke frequency response service to be implemented for the benefit of both the GB grid and the asset owners.

Additionally, this paper presents the modular FESS model developed in MATLAB/Simulink that can provide fast application-based simulation including flexibility to analyse a range of different frequency response services rapidly. This model presents a significant advancement in FESS simulation due to its fast processing time and modular constructions.

The results presented here have the potential to shape the future direction of frequency response services by showing that it is possible for energy-limited assets such as flywheels to participate and provide excellent techno-economic performance, opening up an entirely new discussion around the potential of underutilised energy storage technologies to be deployed for this application.

II. BACKGROUND

BESSs are the most widely deployed energy storage medium that provides these services with BESSs either operational, under construction or planned totalling more than 16GW of capacity, compared to an additional 6GW of liquefied and compressed air, pumped hydro, flywheels and gravity-based technology [13]. Crucially, they generally have a high energy capacity enabling them to provide the services for extended periods of time, therefore generating income over greater durations [14]. Additionally, for the new response services, there are stringent state of energy (SOE) requirements that must be met in order to participate, meaning shorter term energy storage is now unlikely to be able to participate in the frequency service market.

The major downside of Li-ion batteries is their susceptibility to cycle based degradation. It is for this reason that Li-ion systems are often specified with narrow tolerances for operational regions where operating the system outside of these zones will result in rapidly decreasing lifetime of the BESS. Factors such as C-Rate, temperature, energy throughput, Depth of Discharge (DOD), and SOC have all been shown in literature to have significant impacts on battery lifetime [15], [16]. BESSs are generally considered to reach end of life when their capacity falls to 80% of the original capacity.

The primary characteristic that makes a FESS suitable for this set of research is its excellent resistance to cycle-based degradation. Various pieces of literature have quoted the cycle lifetime of flywheels to be anywhere between 10,000 to 1,000,000 full charge discharge cycles before failure [17], [18]. The main method of degradation within a FESS is the wear on mechanical bearings (where present) although this is reversible with regular, inexpensive maintenance [19]. In terms of calendar lifetime, a figure of 20 years is the most often quoted statistic but this can vary based on manufacturers specifications and warranties.

Another commonly discussed feature of FESSs is their high levels of self-discharge, often referred to as spinning losses. With no outside intervention, a flywheel will lose between 20-100% of its stored energy over the course of a day [20], [21]. It is for this reason that flywheels are generally most suited to applications where there will be frequent charge/discharge operations enabling it to spend as little time as possible in an idle state.

Where an ESS is required to charge and discharge frequently the efficiency of the system is an important aspect. Throughout the literature a range of different values for

efficiency are quoted spanning from 80% to over 95%, once again indicating a dependence on manufacturer specific information to be sure of a systems capabilities. However, it is generally agreed within the literature that flywheels do have a high efficiency compared with other mediums [22], [23].

A. STUDY OVERVIEW

The service developed in this paper is represented as a continuous 24/7 service and the effectiveness is determined by the average availability over a year of the service being provided. Availability is defined as the total amount of time where the grid request is met as a proportion of overall operational time. This is presented as 4 in Section IV-D. Additionally, the energy throughput of the service has been assessed and compared with that provided by the existing frequency response services offered by NGEESO in order to verify that the system is operating for a sufficient amount of time to be worthwhile.

The initial analysis is performed on a 1MW/1MWh/1C FESS system providing a 1MW service. A C-Rate sensitivity analysis has been performed to assess the effects of varying the C-Rate on the performance of the system. Finally, a detailed economic analysis is performed showing for the first time a comprehensive picture of how a FESS can be deployed for this application and provide significant economic benefits.

Parts of the study presented in this paper were initially published as part of conference proceedings [12]. The work presented here includes significant new material, including a more detailed methodology, a new literature review, an expanded novel technical analysis and an entirely new novel economic analysis section.

III. LITERATURE REVIEW

As these response services have either only just been introduced or are still being developed, there is a significant gap in completed research. Due to this fact, the closest available literature is that which investigates frequency regulation in general. In terms of a standalone FESS system there is minimal work available. This is due to the generally low energy capacity inherent within flywheels along with the proven track record of BESSs meaning this area is not extensively explored.

The majority of implementations of FESSs for this application consist of systems where the FESS is hybridised with a BESS, such as in [24] which presents a significant extension of operational battery life when hybridised with a FESS. A similar conclusion is reached in [25] which looks at a hybrid configuration providing frequency reserve services, showing an extension of life of 6 years for a hybrid system compared to standalone BESS.

Specifically relating to the new suite of services, the main piece of completed research comes from [7] with a sensitivity study looking into the required C-Rates for provision of the range of new services. This paper determined that DC is generally a less demanding service than DFR, and that higher C-Rates (up to 10C) could be utilised effectively to provide

the service. This suggests that there is a significant opportunity for short term energy storage such as flywheels to provide this service. However, when considering the contract service delivery terms of DC the paper suggests that the higher c-rate systems struggle with maintaining compliance due to long duration frequency events where there is not enough energy in the ESS.

Additionally, [26] takes a more market focused approach to analysing BESSs being utilised for provision of DC. Rather than looking at technical performance, the study looks at the potential economic value in utilising a BESS for this purpose, concluding that a positive economic impact can be achieved. However, it is to be expected that BESSs will be able to adequately perform this service as they are the primary medium that DC has been designed for, and hence there still remains a gap for meaningful research into the performance of energy limited assets.

It is clear from the research conducted that under the current requirements, very short duration energy storage will still be unable to meaningfully participate in the frequency response service market. The work contained in this paper builds upon this conclusion, looking specifically into the operation of FESS when considering no operational restrictions and using this as a basis to develop a service that can be effectively provided by very short duration energy storage without complex state of energy requirements opening up the opportunity for a much wider range of ESS mediums to provide such services.

IV. FLYWHEEL MODEL

In this section, a detailed overview of the MATLAB/Simulink model that has been developed is presented. The most important element of the model and one of its key advantages is the modular subsystems with which it can be built. This enables it to be easily switched from one scenario to another with minimal overall adjustments, thus representing a significantly improved timescale from conceptualisation of a scenario to producing accurate results. Whilst the core components of the model are built from simple blocks from the main Simulink library, they have been brought together in a way that adds further complexity without sacrificing computational speed.

The developed model can simulate a year of frequency response provision at a 1-second time step in 2m 30s, allowing for rapid data collection over a variety of scenarios (*PC specifications - Intel Core i7-6700k CPU @ 4GHz*). Other applications such as wind generation support and solar generation support can be simulated over the same duration and time-step in 5m 48s and 3m 24s respectively.

The model presented in this section is set up to perform analysis on a frequency response service. Where variables are named within the following sections and the related figures, example values are shown in Table 1. Where applicable, values have been taken from technical specifications provided by a flywheel manufacturer.

Each figure in the following section contains indicators illustrating where the signals from different blocks of the

TABLE 1. Variables used in Fig. 2-6 when studying a 1MWH/5C FESS delivering a 1MW service with an availability payment of £1.83/MW/HR.

Variable Name	Value	Variable Name	Value
ExportLoss	0.05	InitialFESS_SOC	50
ImportLoss	0.05	FESSC	5
FESSChargeEf	0.95	SpinLoss	0.001
FESSDischargeEf	1.05	Service	1000
FlywheelCapacity	1000	Apayment	1.83

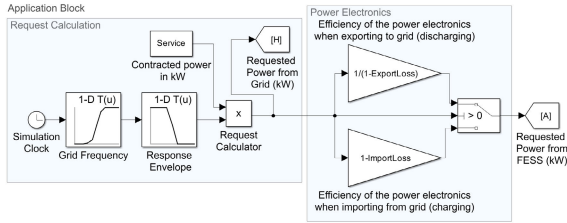


FIGURE 2. Application block from simulink model.

model are sent to and from. The main modular components are detailed below;

A. APPLICATION BLOCK

This block is modified according to the simulated application. It will consist of whatever components are necessary to generate a power-request signal to the FESS. For delivery of frequency response for example, this would consist of an input of second-by-second frequency data that can then be converted into a power request using a lookup table populated to provide the required response envelope. By modifying the points in the lookup table the FESS can be set to provide different services such as DC, DR and DM. The power set points formulated in this study are utilised to set the response envelope within this lookup table. The output of this block is a request to the FESS in kW. The application block as used in a frequency response simulation is shown in Fig. 2.

It also contains a system which represents the inverter, calculating the losses experienced by the power electronics present in the system, accounting for these losses by either increasing the request in a discharge scenario or decreasing the request in a charge scenario so that the input/output demand to the FESS is accurate. These values are set as decimal values, for instance, if a 95% efficiency on export was utilised, the value of ExportLoss in Fig. 2 would be set to 0.05.

B. CONTROL BLOCK

This block consists of a MATLAB function block that controls how and when the FESS charges or discharges. The inputs are power request, the state of charge (SOC) at the given time step and any required FESS specifications such as capacity, C-Rate and SOC limits which can either be specified as inputs taken from the rest of the model, or within the MATLAB function. The outputs will be charging power and discharging power in kW.

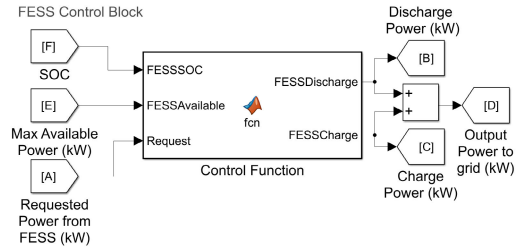


FIGURE 3. Control block from simulink model.

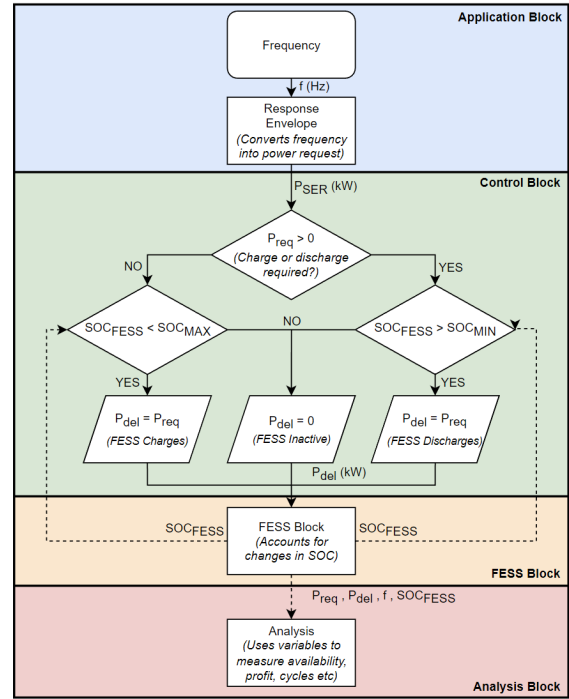


FIGURE 4. Control strategy overview.

The Simulink extract is shown in 3, with the function block code represented diagrammatically in Fig. 4. The function determines whether the request is for charge or discharge, and then determines whether the FESS is within the required SOC range to respond to the request. If this is true, then the corresponding charge or discharge power is output from the function, whilst if it is not true then the output of both ports is zero.

C. FESS BLOCK

The block representing the FESS forms a closed loop with the control block, receiving its input as a charge/discharge power from the control block before feeding its output of an updated SOC back to it for the next second of the simulation. An overview of this block is shown in Fig. 5.

The flywheel itself is modeled using the ‘Bucket model’ approach, also commonly referred to as a ‘Power-energy model’. This represents the energy storage as a ‘bucket’ to which energy is added and removed to simulate charging and discharging. This approach is based on 1 where E_t is the

TABLE 2. Flywheel specifications.

Specification	Value	Specification	Value
Rated Energy	7.5kWh	Rated Power	60kW per unit
C-Rate	8C	Material	Steel
Cycle capacity	500,000	Cost	£750/kW
Response time	5ms	Efficiency	95%

energy stored within the flywheel at time t in kWh, P_t is the instantaneous charge/discharge power delivered by the flywheel at time t in kW, with this value divided by 3600 to convert from kW/second to kWh. When discharging, P_t will be negative and therefore the energy will be subtracted from E_{t-1} whilst when charging this value will be positive.

$$E_t = E_{t-1} + \frac{P_t}{3600} \quad (1)$$

In the ‘Flywheel’ section, the energy capacity and the initial SOC are used to determine the initial level of stored energy within the integrator block. This block is then updated each time step with the instantaneous charge/discharge power as given in 1, which is adjusted according to the charge/discharge efficiency blocks. It is then converted to a SOC, where it is then used for the next time step within the control block.

Spinning losses are calculated as a % SOC loss per second but only for simulation steps where the flywheel is idle, with a switch case block determining whether charge/discharge power is being delivered before removing the given spinning loss for that 1-second period if the flywheel is idle.

Cycles are counted by determining the difference between the current time step SOC and the previous time step SOC to produce an equivalent partial cycle (EPC) as shown in 2. This is then summated with every cumulative 100% of SOC change being counted as one cycle as shown in 3.

$$EPC = \frac{dSOC}{100} \quad (2)$$

$$Cycles = \int_0^t EPC \quad (3)$$

The parameters of the system have been taken from technical specifications provided by a flywheel manufacturer and are detailed in Table 2. The flywheel is a horizontal axis steel modular FESS, installed either individually or as sets of 8 flywheels per container. The frequency data utilised within this work covers the period from November 2020 to October 2021 and was sourced from National Grid at a resolution of 1s [27].

D. METRIC BLOCK

This block takes inputs from the other blocks and converts them into metrics for export and assessment. In this scenario, it focuses on calculating the average availability for each 30-minute period of operation and the payment based on this value. The power electronics system accounts for the reverse of the calculation performed within the application block

to ensure that the ‘grid’ power seen is correct. Total cycles are calculated using 3 as an integrator block, whilst average SOC and average availability are integrated and divided by simulation time to give average values.

The availability is calculated using a MATLAB function implementing 4 over rolling 30-minute periods, where P_{req} is the power requested by the service, P_{del} is the power delivered by the ESS, and t_{end} is period of operation. The memory block stores the count of non-available time-steps and at the end of each 30-minute period, this value is reset. This is achieved using the code included in Fig 7.

$$A_v(\%) = \frac{\sum_{t=0}^{t_{end}} x}{t_{end}} \begin{cases} x = 1 & P_{del} = P_{req} \\ x = 0 & \text{otherwise} \end{cases} \quad (4)$$

The payment calculator system takes the service level, the availability payment in £/MW/hr and a 30-minute step counter as inputs to a function block. At the end of each 30-minute period the average availability is used to determine the level of payment given, which is continuously summed using the integrator block. This replicates 5 to produce a value for C_r where A_f is the clearing price in £/MW/hr, P_{SER} is the service level in kW and P_f is the ratio that determines payment based on the availability of the system. This is achieved using the code included in Fig. 8.

$$C_r = 0.5A_fP_{SER}P_f \begin{cases} A_v > 95\% & P_f = 1 \\ 60\% < A_v < 95\% & P_f = 0.75 \\ 10\% < A_v < 60\% & P_f = 0.5 \\ A_v < 10\% & P_f = 0 \end{cases} \quad (5)$$

V. CREATING A BESPOKE RESPONSE SERVICE

The main metric for measuring an ESS’s ability to provide a frequency response service is termed ‘Availability’ and was previously defined in 4. This metric is utilised for payment purposes in existing frequency response services, with reducing payments as the availability drops below 95%.

For this reason, the target for an effective service is that it should be available for a minimum of 95% of the operational time. However, the service should also be able to reach this availability at higher C-Rates with many of the existing or in-development FESSs having C-Rates in the region of 4-20C. It should also provide a total energy throughput in the same order of magnitude as that which would be provided by existing services, which has been chosen as a design criterion to ensure that the service is operating frequently enough to contribute meaningfully to the balancing mechanism.

The initial analysis is performed on a 1MW/1MWh/1C FESS providing a 1MW service followed by a C-Rate sensitivity analysis to assess the effects of varying the C-Rate on the performance of the system. C-Rate is given as in 6 where E_{ESS} is energy capacity in kWh and P_{ESS} is rated power in kW. In basic terms, it refers to the power-to-energy ratio of the ESS and can be used to effectively compare different storage mediums.

$$C_{rate} = \frac{P_{ESS}}{E_{ESS}} \quad (6)$$

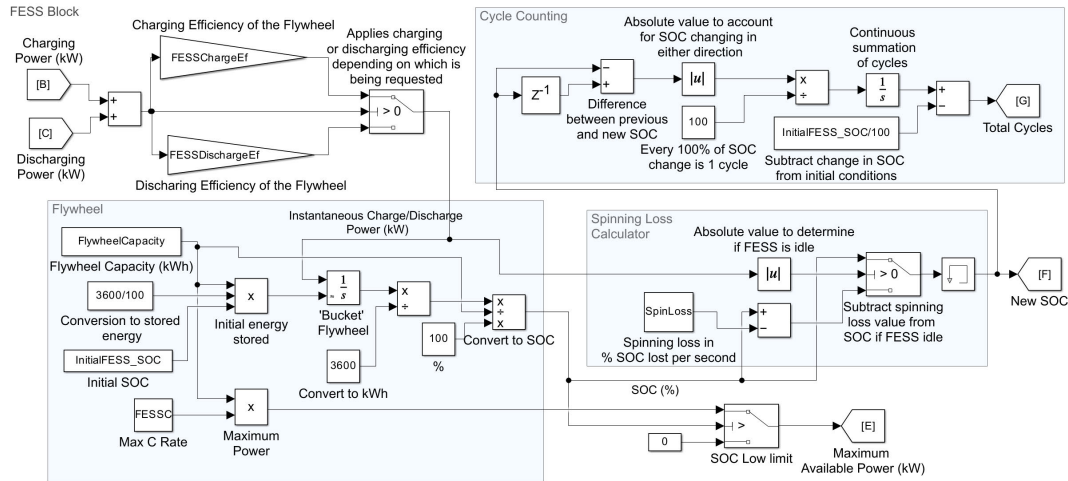


FIGURE 5. FESS block from simulink model.

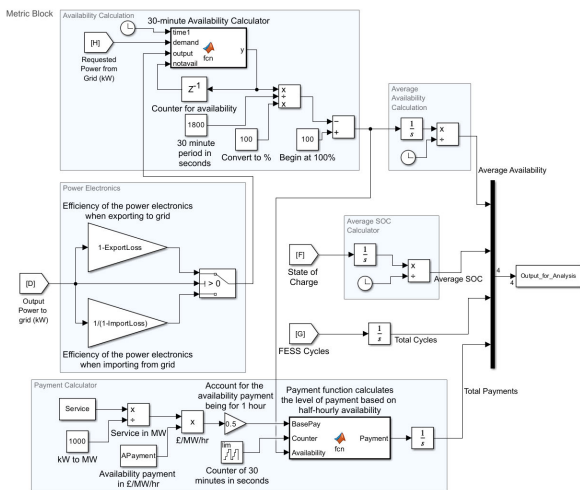


FIGURE 6. Metric Block from Simulink model.

```
function y = fcn(time1,demand,output, notavail)
if (rem(time1,1800) == 0) % reset the counter
    % after each 30 minute period
    notavail = 0;
end
if (demand ~= output) % if demand does not match FESS output,
    % add one to the not-available counter
    y = notavail+1;
else
    y = notavail; %if demand matches FESS output, do not add one
    %to the not-available counter
end
```

FIGURE 7. Code excerpt for availability calculation in Fig. 6.

A. INITIAL ANALYSIS

The initial analysis of a bespoke frequency response envelope consisted of varying the 100% power point (P_1 and P_{-1} on Fig. 9) for both the low and high frequency ends of the spectrum with a 1MWh/1MW/1C system providing a 1MW service. The ‘knee points’ P_k and P_{-k} are not used in this initial analysis with the service being a linear rise from 50Hz and zero power in either direction resulting in a straight line

```
function Payment = fcn(BasePay,Counter,Availability)
% Implementation of Equation 4
if(Counter == 1799 && Availability<10)
    Payment = 0;
elseif(Counter == 1799 && Availability>=10 && Availability<60)
    Payment = BasePay*0.5;
elseif(Counter == 1799 && Availability>=60 && Availability<95)
    Payment = BasePay*0.75;
elseif(Counter == 1799 && Availability>=95)
    Payment = BasePay;
else
    Payment = 0;
end
```

FIGURE 8. Code excerpt for payment calculation in Fig. 6.

with no breakpoints. A year-long simulation was conducted for each combination between 49.5–49.9Hz and 50.1–50.5Hz. The results of this simulation are shown in Fig 10.

It is immediately apparent that as the 100% power point is moved further from 50Hz in both directions the average availability steadily increases. From a symmetrical 49.9/50.1Hz combination giving an average availability of 91.2%, the combination of 49.5/50.5Hz provides an average availability of 97.4% showing a significant improvement.

There is also a degree of asymmetry to the results, with a higher availability produced when the high frequency 100% power point is reached sooner than the low frequency 100% power point. This leads to the maximum availability of 98.5% being achieved with a combination of 49.5Hz and 50.44Hz. However, if the asymmetry is increased too far then the average availability experiences a rapid reduction.

This asymmetry is due to the FESS experiencing spinning losses. By having a steeper charging curve, the spinning losses are constantly being countered with more energy being taken from the grid than discharged back. In this manner, the response envelope being slightly asymmetric uses the spinning losses to its advantage.

Taking this assessment as a baseline, the best performing 100% power point combination was used to perform a C-Rate sensitivity analysis. The C-Rate was increased incrementally

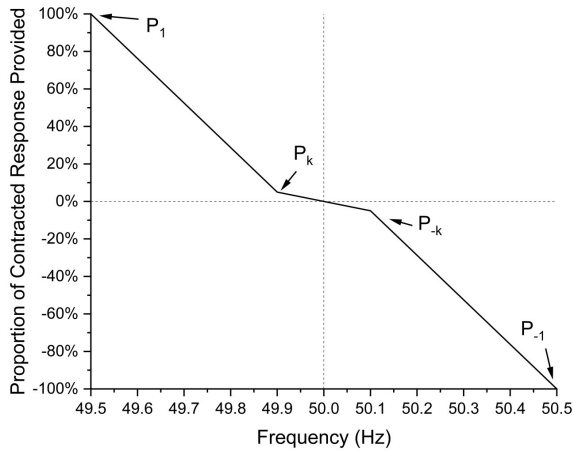


FIGURE 9. Response envelope example showing the points in the envelope that are varied within this study.

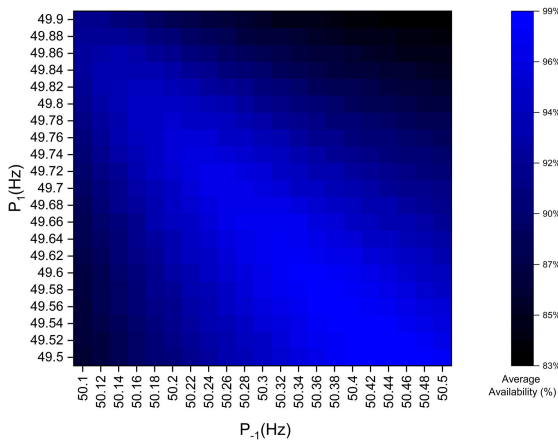


FIGURE 10. Average availability for varying high and low frequency 100% power points.

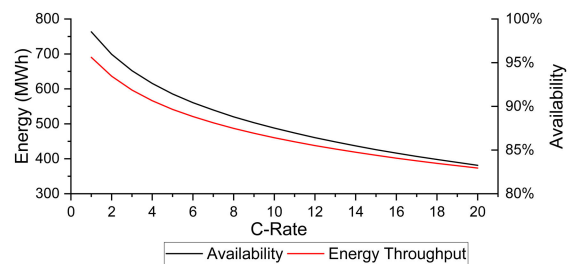


FIGURE 11. C-Rate sensitivity analysis when utilising 100% power points of 49.5/50.44Hz with a 1MW/1MWh/1C FESS providing a 1MW service.

up to a value of 20C with the results of this analysis shown in Fig. 11. There is a significant drop in average availability as the C-Rate is increased, with only a 1C and 2C system achieving average availability in excess of the required 95%. This suggests that the suitability of the envelope to more common FESS system characteristics like high power and low energy is poor and needs further tuning to enable it to perform at higher C-Rates.

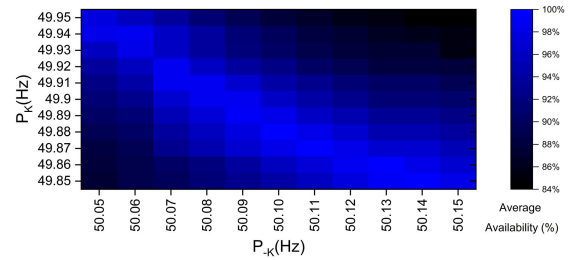


FIGURE 12. Heatmap of average availability for varying combinations of high and low frequency knee points.

Also in Fig. 11 is the total energy throughput of each individual system in MWh. This metric is intrinsically tied to that of availability, but the key aspect to note is that even for a 20C system the energy throughput is still significant with 373.6MWh passing through the FESS over the course of a year. Compared to the results previously discussed in [12], at its peak of 690.39MWh for a 1C system the service will see more usage than all current services bar DR, with a very similar energy throughput to DFR but with an extra 1.1% availability across the year, showing that the refinement of the service to the flywheels advantages is working to enable it to provide a more reliable service than existing ones.

B. KNEE POINT ANALYSIS

Both DC and DM have ‘Knee Points’ where up to a certain frequency the power delivery is a small proportion of the overall contracted service, followed by a linear rise to the maximum power point. This section of the study focuses on placing a knee point into the response envelope and how this effects the average availability.

The maximum power points are set as 49.5Hz and 50.44Hz (points P1 and P-1 respectively on Fig. 9) as determined in the previous section, with the power level of the knee-point set as 0.05% of the overall contracted service, replicating the setting used by DC and DM. The low and high knee-point frequencies (points Pk and P-k on Fig. 9) are then varied between 49.85-49.95Hz and 50.05-50.15Hz respectively in increments of 0.01Hz. The results of this analysis are shown in Fig 12.

The average availability once again increases as the knee-point is moved further away from 50Hz before decreasing again after a peak at 49.91/50.09Hz. In 90% of simulated combinations, the average availability was reduced by adding in a knee point. Despite this, some of the combinations represent a significant increase in average availability, peaking with the combination of knee points at 49.87Hz and 50.12Hz which provides an average availability of 99.89% across the year, meaning it will fail to meet the requested power of the grid for less than 10 hours over the course of the year. This combination shows again the benefits of small asymmetry within the response envelope, causing the FESS to charge slightly more often than it discharges.

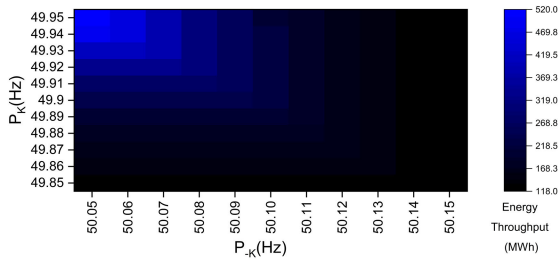


FIGURE 13. Heatmap of energy throughput for varying combinations of high and low frequency knee points.

TABLE 3. Final bespoke response envelope settings for 1C system utilising a knee point approach.

Frequency	Power Point
49.5	1
49.87	0.05
49.985	0
50.015	0
50.12	-0.05
50.44	-1

The total energy throughput for the year was also monitored during this assessment, with the values ranging from 518.4MWh (49.95/50.05Hz knee points) to 118.1MWh (49.95/50.15Hz knee points) as shown in Fig. 13.

For the combination that provided the highest average availability (49.87/50.12Hz), the total energy throughput was 160.9MWh, which would place it between the levels of energy provided by DM (83.9MWh) and DC (371.0MWh) as previously detailed in [12]. This suggests that it operates sufficiently over the course of a year to be providing a worthwhile service to the GB Grid.

The final knee point settings for the bespoke envelope have therefore been set at 49.87/50.12Hz, combined with the earlier high point settings of 49.5/50.44Hz to create the final bespoke envelope, with these details presented in Table 3. The response envelope created is most closely aligned with the existing DC service, but with knee points that cause higher power to be delivered at an earlier frequency threshold in both positive and negative directions.

Fig. 14 shows the simulation output of a 1MW/1MWh/1C FESS providing this service. Frequency data taken from National Grid at 1s resolution was used for this simulation [27]. The ability of the FESS to provide this service can be seen in the regular small discharge and charge events interspersed with occasional high-power responses, maintaining a stable SOC throughout the day.

Following on from introducing a knee point, a second C-Rate sensitivity analysis was conducted with the results of this shown in Fig. 15. Compared with the analysis shown in Fig. 11 there is a much more shallow reduction in availability as the C-Rate is increased. At 10C (0.1MWh/1MW) there is still an average availability above 95% whilst still providing 138.54MWh of energy throughput across the year, showing

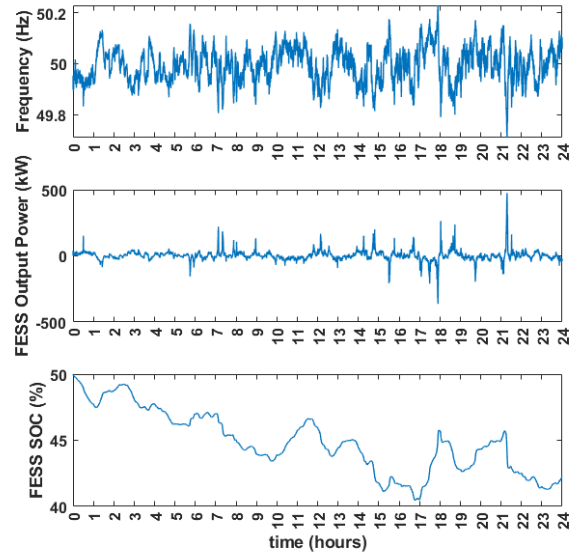


FIGURE 14. 1MW/1MWh/1C FESS providing a 1MW service under the bespoke response profile for 1 day in December 2020 using 1s resolution frequency data.

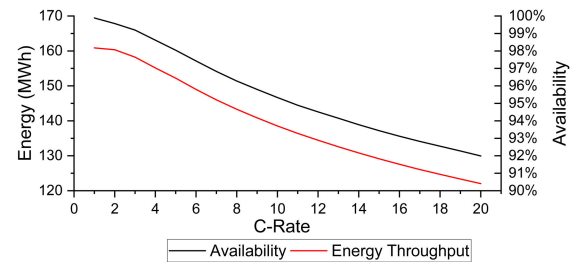


FIGURE 15. C-Rate sensitivity analysis when utilising the bespoke response envelope.

that it is possible to have a high power, low energy FESS that can provide an effective frequency response service which is critical in allowing the more common specifications of FESS to operate in the frequency response service market.

Again, Fig. 15 also shows the energy throughput across the year. This time, in contrast with Fig. 11, the energy throughput stays in a much narrower range across all studied C-Rates with the lowest throughput being for a 20C system (122.04MWh) and the highest being for a 1C system (160.87MWh). The closest base service in terms of energy throughput is DC with a value of 83.9MWh (as detailed previously in [12]), and crucially when compared to the bespoke designed service there is an improvement of 2.49% availability (from 97.8% to 99.89%) whilst providing almost double the energy throughput. This is an excellent indicator of the advantages gained from designing a service specifically for a FESS or other very short duration storage rather than treating all ESS mediums as equal.

Fig. 16 shows the number of cycles experienced per year under the initial response envelope discussed in Section A and under the subsequent envelope discussed in this section.

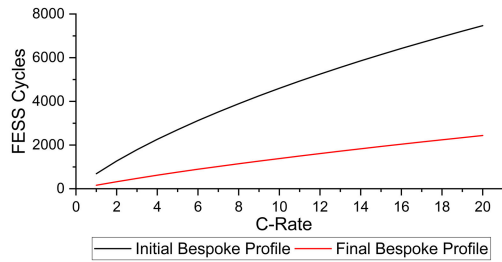


FIGURE 16. Cycles experienced by the FESS under the initial and final response envelope for varying C-Rates.

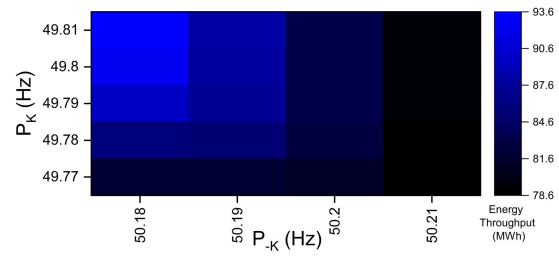


FIGURE 18. Excerpt of energy throughput based knee-point optimisation for a 5C system.

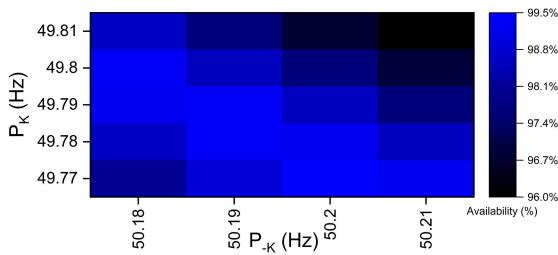


FIGURE 17. Excerpt of average availability based knee-point optimisation for a 5C system.

TABLE 4. Results of C-Rate based optimisation of the response envelope knee points including average availability for each configuration when performing DC High/Low.

C-Rate	Low Knee Point (Hz)	High Knee Point (Hz)	Availability	Energy (MWh)	DC Availability
1	49.87	50.12	99.89%	143.88	99.18%
5	49.78	50.19	99.34%	85.20	92.22%
10	49.79	50.18	97.80%	85.63	88.04%
15	49.80	50.17	95.93%	85.68	85.44%
20	49.78	50.18	95.00%	76.05	83.40%

When comparing how the two response envelopes translate into FESS cycles, it is clear that at higher C-Rates the amount of cycling required by the FESS may be prohibitive even for a cycle resistant storage medium such as flywheels. Taking the lower end of the quoted spectrum of cycle limits as 100,000 cycles, this would mean that all systems with a C-Rate of 9C and above would likely require replacement before the required 25 year lifespan was achieved (4,254 cycles per year for 25 years would result in 106,350 cycles experienced for a 9C system). Of course it is important to note that many manufacturers quote the cycle life for FESSs as unlimited, in which case this would cease to be an issue.

Looking at the final bespoke profile however, all of the C-Rates studied would comfortably fall below even this lower limit, with the maximum value of 2,439 cycles per year resulting in just 60,975 cycles. It is clear that at this level of cycling more traditional ESSs such as Li-ion BESSs would not be able to deliver the same service as they are most often quoted with a maximum cycle life of 10,000.

C. HIGHER C-RATE ANALYSIS

A final study was conducted to optimise the response envelope for different FESS C-Rates. The key criteria was achieving the highest availability possible whilst attempting to match, or improve upon, the lowest energy throughput provided by an existing service (83.9MWh - DC) [12]. An example of how this was conducted for a 5C system is shown in Fig 17 and Fig 18.

This analysis showed that whilst the average availability can be increased further, the energy throughput would then be decreased further. The combinations where the energy

throughput falls below the desired level are discounted, with the highest availability from the remaining combinations taken as the best option. This optimisation balances the two to provide the most suitable overall service for each C-Rate. It should be noted however that if energy throughput was removed as a constraint then further increases in average availability could be achieved, albeit with the system providing less energy to and from the grid. For instance, in Fig 17 and Fig 18, a higher average availability could be achieved using the combination of 49.77/50.2Hz but would result in a loss of 4.03MWh of energy throughput across the year, for just a 0.13% increase in average availability.

The results of the study for a 5C, 10C, 15C and 20C system are shown in Table 4, with the 1C results determined previously included for reference.

These results show that for different C-Rates slight variations on the high and low knee points are required to extract the best combination of average availability and energy throughput. By tailoring the knee points to the C-Rate being considered, a 20C system was able to achieve a 95% availability, albeit with a slightly lower energy throughput than desired. The outcome of this study shows that with a small amount of versatility in response envelope, much higher C-Rate systems can provide standalone frequency response services.

The key conclusion to be drawn from Table 4 is when comparing the average availability achieved under the bespoke profile with the availability achieved when performing the combined DC high and low service. Whilst there is minimal improvement at the 1C configuration, it is in the more commonly found higher C-Rates that the true breakthrough of this research is realised. For a 20C FESS, the average

TABLE 5. Availability for varying FESS C-Rates across differing years of frequency data using response envelopes from Table 4.

C-Rate	2019	2020	2021	2022	2023	Average
1	99.86%	99.71%	99.83%	99.75%	99.83%	99.80%
5	99.29%	99.09%	99.42%	99.54%	99.41%	99.35%
10	97.06%	96.98%	97.25%	97.98%	97.49%	97.35%
15	95.26%	95.83%	95.20%	96.21%	95.79%	95.69%
20	94.62%	94.77%	94.63%	95.28%	95.01%	94.86%

availability that it can provide whilst running 24/7 is 11.60% higher for the bespoke profile jumping from 83.40% to 95%. Across all of the higher C-Rate systems studied, the FESS can now provide a much more reliable and worthwhile service all whilst delivering levels of energy throughput either in excess of or very close to that provided by a 1C system delivering DC High/Low.

The bespoke envelope has been optimised for the frequency data from November 2020 to October 2021. Variations in frequency data from one year to the next could lead to differences in average availability, therefore to increase confidence in the developed response envelope the profiles determined in Fig. 4 were simulated over 5 years of frequency data. This allows an assessment to be made on the designed profiles suitability for ongoing services and allows for greater confidence in the bespoke profiles suitability when accounting for year-to-year variation. In Table 5 it is shown that similar levels of availability are maintained across the 5 years analysed. The results show that the designed profiles hold these levels of availability across multiple years, with an expected variance from year to year that is minimal. The average availability over 5 years for a 20C system experiences the biggest variance from that produced in Table 4, with a small drop from 95% to 94.86%.

VI. ECONOMIC CASE STUDY

For the economic analysis, the following assumptions have been made to ensure the study falls in line with real world conditions and maintains consistency with other studies conducted in this area such as [28];

- It is assumed that the payment mechanism will be made on a sliding scale with full payment for half-hour periods where the availability exceeds 95% and reduced payments below this. This is a reasonable assumption as it is unlikely that a bespoke payment mechanism for this service would be worthwhile.
- The availability payment will be calculated as a value of £/MW/hr, replicating the current arrangement for existing services.
- The average clearing price for availability payments will be within the same range as found within the market in recent conditions. The average clearing price over 2023 for DC, DM and DR was £1.83/MW/hr [29].
- Discount rate is set as 8%. The discount rate has been set to a higher value to represent a slightly higher risk level of the investment.

- Each FESS system uses the optimum settings for the response envelope outlined previously in Table 4.
- Where a FESS Total Capital Cost (TCC) is set as a fixed value, it has been set to £780/kW in line with previous findings from this work [3].

NPV has been calculated using 7 where $C_{investment}$ is the initial investment in the system, C_r is the yearly income (£) as determined in 5, N is the system lifetime in years and d is the discount rate [30].

$$NPV = \sum_{n=1}^N \frac{C_r}{(1+d)^n} - C_{investment} \quad (7)$$

The main objective of this section is to analyse the required level of availability payment that would result in a typical FESS system achieving a positive Net Present Value (NPV) under current economic conditions. Using the same approach as the previous section, the systems studied will consist of a 1MW FESS with varying C-Rates between 5C and 20C to reflect typical FESS systems.

When considering these results it is important to contextualise them by comparing with values produced in similar studies. In [31], which looks at a combined wind battery system providing frequency response, shows the system achieving a NPV of £7.865m with a discount rate of 8%. Values varying between £1-40m NPV are achieved in [32], which looks at the optimal placement of BESS within the UK to provide frequency response services. Finally, in [33], a BESS providing a frequency response service is able to achieve NPV in the region of £12.9-18.2m when operating in an isolated power system.

To investigate the effect of the current economic conditions on the viability of a FESS for delivering the bespoke service, a sensitivity analysis was performed to determine the highest Total Capital Cost (TCC) at which the system could provide a positive NPV. To do this, the availability payment was set as £1.83/MW/hr in line with the average clearing price for 2023. The TCC is then varied between £200/kW and £5,000/kW and the results are shown in Fig. 19

Across a significant range of TCC values, all four different FESS configurations can provide a significantly positive NPV under these conditions. The highest threshold value is £4,159/kW for a 5C system providing a positive NPV, which means any system cheaper than this will produce in excess of 8% return on investment. The lowest threshold on the other hand is still a value of £3,364/kW for a 20C system. In previous works the average TCC of a FESS has been found to be £780/kW [3], and at this value the NPV achieved ranges between £3.38m for a 5C system to £2.58m for a 20C system, values which fall within the range expected from other studies discussed earlier in this section. The 10C and 15C systems achieve an NPV at £780/kW TCC of £3.08m and £2.75m respectively.

Following on from this, the TCC of the system was set at £780/kW, and the clearing price varied between £0.01/MW/hr and £3/MW/hr to determine how resistant the designed

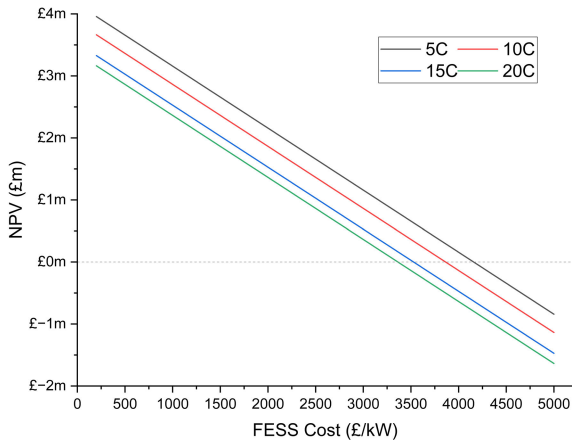


FIGURE 19. Sensitivity analysis on varying FESS TCC and C-Rate for bespoke response profile.

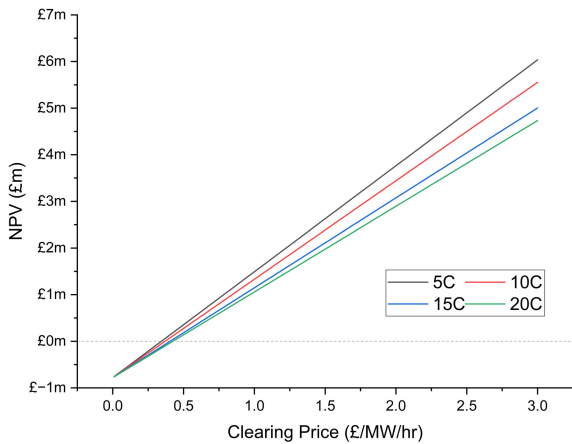


FIGURE 20. Sensitivity analysis on varying clearing price and C-Rate for bespoke response profile.

profile would be to variations in the clearing price. The results of this analysis are shown in Fig. 20.

Fig. 20 shows that a 5C system performing the profile determined in Table 4 would produce a positive NPV at any clearing price above £0.35/MWh/hr, with a 20C system requiring clearing prices above £0.43/MWh/hr. The 10C and 15C systems achieve a positive NPV at £0.37/MWh/hr and £0.41/MWh/hr respectively. This shows that the designed profiles would be able to provide a positive economic performance even at much lower clearing prices than experienced in recent years. This leads to the conclusion that there is significant potential for a large range of FESS costs and configurations that can be deployed to provide positive economic results.

Finally, a sensitivity analysis was performed on the frequency data utilised for this study. As in Table 5, frequency data was used for years 2019 to 2023 with an NPV analysis carried out for a FESS with a TCC of £780/kW and a clearing price of £1.83/MWh/hr. Fig. 21 shows that for the four C-Rates studied, there is a small variation from year to year,

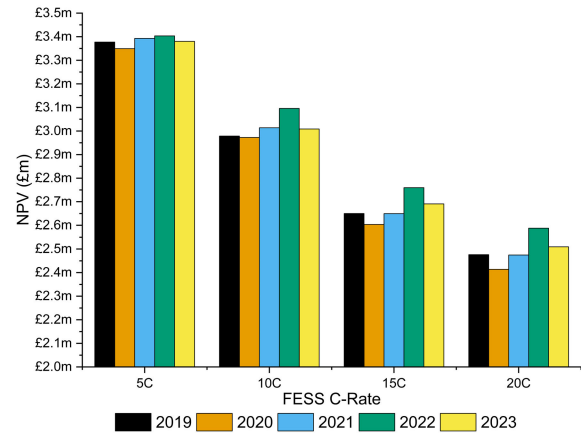


FIGURE 21. Sensitivity analysis on varying years of frequency data for bespoke response profile with a TCC of £780/kW and clearing price of £1.83/MWh/hr.

with 2022 producing the largest NPV and 2020 producing the smallest. The yearly variation for each C-Rate is minimal, with the greatest variation between the minimum and maximum NPV achieved being £0.17m for a 20C system, whilst for a 5C system this variation is £0.05m. This suggests that utilising different frequency data periods does not significantly impact the expected techno-economic performance of the systems considered in this study.

VII. CONCLUSION AND FUTURE WORK

In this study, a novel FESS model has been introduced and detailed, showing the modular arrangement that enables rapid simulation of varying applications. This model has then been utilised to design a bespoke frequency response service. When considering a baseline 1MW/1MWh/1C system providing a 1MW service, a peak average availability of 99.89% can be achieved when delivering the bespoke envelope detailed in Table 3.

Subsequently, this response envelope has been investigated for different FESS C-Rates. It has been shown that different FESS C-Rates require slightly different response profiles in order to extract maximum performance benefits. By using these small modifications to the response profile, a 20C FESS can achieve an average availability of 95%.

Finally, the economic implications were assessed showing that a FESS delivering the bespoke profile can provide a positive NPV up to a TCC of between £3,364 and £4,159 depending on the C-Rate of the system. Additionally, at the current market TCC of a FESS and recent ancillary service market conditions, a 5C FESS can provide an NPV of £3.38m. The NPV that was achievable under varying scenarios was shown to be competitive with values found in literature for BESSs. It was also shown that when delivering the bespoke profiles, a 5C FESS could provide a positive NPV at a clearing price as low as £0.35/MWh/hr.

The research presented in this study has the potential to open up the frequency response market to a much

wider range of energy storage mediums such as FESSs and Super-capacitors than has been previously been suggested. Future works should build upon these results, looking into the potential impact on the stability of the grid from large-scale deployment, as well as exploring bespoke profiles for other storage technologies.

REFERENCES

- [1] National Grid ESO. (2021). *Firm Frequency Response (FFR) Post Tender Reports*. [Online]. Available: <https://data.nationalgrideso.com/ancillary-services/firm-frequency-response-post-tender-reports>
- [2] B. Gundogdu, D. Gladwin, and D. Stone, "Battery energy management strategies for U.K. firm frequency response services and energy arbitrage," *J. Eng.*, vol. 2019, no. 17, pp. 4152–4157, Jun. 2019.
- [3] A. J. Hutchinson and D. T. Gladwin, "Standalone and hybridised flywheels for frequency response services: A techno-economic feasibility study," *Energies*, vol. 17, no. 11, p. 2577, May 2024. [Online]. Available: <https://www.mdpi.com/1996-1073/17/11/2577>
- [4] J. Meng, Y. Mu, H. Jia, J. Wu, X. Yu, and B. Qu, "Dynamic frequency response from electric vehicles considering travelling behavior in the Great Britain power system," *Appl. Energy*, vol. 162, pp. 966–979, Jan. 2016.
- [5] M. Cheng, J. Wu, S. J. Galsworthy, N. Gargov, W. H. Hung, and Y. Zhou, "Performance of industrial melting pots in the provision of dynamic frequency response in the Great Britain power system," *Appl. Energy*, vol. 201, pp. 245–256, Sep. 2017, doi: [10.1016/j.apenergy.2016.12.014](https://doi.org/10.1016/j.apenergy.2016.12.014).
- [6] National Grid ESO. (2024). *New Dynamic Services (DC/DM/DR)*. [Online]. Available: <https://www.nationalgrideso.com/industry-information/balancing-services/frequency-response-services/new-dynamic-services-dcdmdr>
- [7] A. Abdulkarim and D. T. Gladwin, "A sensitivity analysis on power to energy ratios for energy storage systems providing both dynamic firm and dynamic containment frequency response services in the U.K.," in *Proc. 47th Annu. Conf. IEEE Ind. Electron. Soc. (IECON)*, Oct. 2021, pp. 1–6.
- [8] A. J. Hutchinson and D. T. Gladwin, "Suitability assessment of flywheel energy storage systems for providing new frequency response services in the U.K.," in *Proc. IEEE PES Innov. Smart Grid Technol. Asia (ISGT Asia)*, Nov. 2022, pp. 495–499.
- [9] K. Yan, G. Li, R. Zhang, Y. Xu, T. Jiang, and X. Li, "Frequency control and optimal operation of low-inertia power systems with HVDC and renewable energy: A review," *IEEE Trans. Power Syst.*, vol. 39, no. 2, pp. 4279–4295, Mar. 2024.
- [10] S. Fazal, M. E. Haque, M. T. Arif, A. Gargoom, and A. M. T. Oo, "Grid integration impacts and control strategies for renewable based microgrid," *Sustain. Energy Technol. Assessments*, vol. 56, Mar. 2023, Art. no. 103069.
- [11] M. W. Siti, D. H. Tungadio, Y. Sun, N. T. Mbungu, and R. Tiako, "Optimal frequency deviations control in microgrid interconnected systems," *IET Renew. Power Gener.*, vol. 13, no. 13, pp. 2376–2382, Oct. 2019.
- [12] A. J. Hutchinson and D. T. Gladwin, "A bespoke frequency response service suitable for delivery by flywheel energy storage systems," in *Proc. IEEE PES Innov. Smart Grid Technol. Conf. Eur. (ISGT-Europe)*, Oct. 2022, pp. 1–5.
- [13] (2021). *Report Shows Huge Scale of U.K. Energy Storage Boom*. [Online]. Available: <https://www.imeche.org/news/news-article/report-shows-huge-scale-of-uk-energy-storage-boom>
- [14] J. Martins and J. Miles, "A techno-economic assessment of battery business models in the U.K. electricity market," *Energy Policy*, vol. 148, Jan. 2021, Art. no. 111938.
- [15] J. Wang et al., "Degradation of lithium ion batteries employing graphite negatives and nickel–cobalt–manganese oxide + spinel manganese oxide positives: Part I, aging mechanisms and life estimation," *J. Power Sources*, vol. 269, pp. 937–948, Dec. 2014, doi: [10.1016/j.jpowsour.2014.07.030](https://doi.org/10.1016/j.jpowsour.2014.07.030).
- [16] C. Liu, Y. Wang, and Z. Chen, "Degradation model and cycle life prediction for lithium-ion battery used in hybrid energy storage system," *Energy*, vol. 166, pp. 796–806, Jan. 2019.
- [17] M. Amiryar and K. Pullen, "A review of flywheel energy storage system technologies and their applications," *Appl. Sci.*, vol. 7, no. 3, p. 286, Mar. 2017.
- [18] M. A. Awadallah and B. Venkatesh, "Energy storage in flywheels: An overview," *Can. J. Electr. Comput. Eng.*, vol. 38, no. 2, pp. 183–193, Spring 2015.
- [19] B. Bolund, H. Bernhoff, and M. Leijon, "Flywheel energy and power storage systems," *Renew. Sustain. Energy Rev.*, vol. 11, no. 2, pp. 235–258, 2007.
- [20] B. Zakeri and S. Syri, "Electrical energy storage systems: A comparative life cycle cost analysis," *Renew. Sustain. Energy Rev.*, vol. 42, pp. 569–596, Feb. 2015, doi: [10.1016/j.rser.2014.10.011](https://doi.org/10.1016/j.rser.2014.10.011).
- [21] J. Liu, C. Hu, A. Kimber, and Z. Wang, "Uses, cost-benefit analysis, and markets of energy storage systems for electric grid applications," *J. Energy Storage*, vol. 32, Dec. 2020, Art. no. 101731, doi: [10.1016/j.est.2020.101731](https://doi.org/10.1016/j.est.2020.101731).
- [22] P. W. Parfomak, "Energy storage for power grids and electric transportation," Congressional Res. Service, Washington, DC, USA, Tech. Rep. NREL/TP-6A20-51252, 2012. [Online]. Available: <https://research-hub.nrel.gov/en/publications/energy-storage-for-power-grids-and-electric-transportation-a-tech>
- [23] C. K. Das, O. Bass, G. Kothapalli, T. S. Mahmoud, and D. Habibi, "Overview of energy storage systems in distribution networks: Placement, sizing, operation, and power quality," *Renew. Sustain. Energy Rev.*, vol. 91, pp. 1205–1230, Aug. 2018, doi: [10.1016/j.rser.2018.03.068](https://doi.org/10.1016/j.rser.2018.03.068).
- [24] S. D. Sessa, A. Tortella, M. Andriollo, and R. Benato, "Li-ion battery-flywheel hybrid storage system: Countering battery aging during a grid frequency regulation service," *Appl. Sci.*, vol. 8, no. 11, p. 2330, Nov. 2018.
- [25] P. Mouratidis, B. Schüßler, and S. Rinderknecht, "Hybrid energy storage system consisting of a flywheel and a lithium-ion battery for the provision of primary control reserve," in *Proc. 8th Int. Conf. Renew. Energy Res. Appl. (ICRERA)*, Nov. 2019, pp. 94–99.
- [26] L. Ochoa-Eguilegor, N. Goitia-Zabaleta, A. González-Garrido, A. Saez-de-Ibarra, H. Gaztañaga, and A. Hernandez, "Optimized market bidding of energy storage systems for dynamic containment service," in *Proc. IEEE Int. Conf. Environ. Electr. Eng. IEEE Ind. Commercial Power Syst. Eur. (EEEIC/I CPS Europe)*, Sep. 2021, pp. 1–6.
- [27] National Grid ESO. (2021). *Historic Frequency Data*. [Online]. Available: <https://www.nationalgrideso.com/balancing-services/frequency-response-services/historic-frequency-data>
- [28] A. J. Hutchinson and D. T. Gladwin, "Techno-economic analysis of a flywheel energy storage system performing a dynamic frequency response service," in *Proc. IEEE 30th Int. Symp. Ind. Electron. (ISIE)*, Jun. 2021, pp. 1–6.
- [29] National Grid ESO. (2024). *Enduring Auction Capability (EAC) Auction Results*. [Online]. Available: <https://www.nationalgrideso.com/data-portal/eac-auction-results>
- [30] (2024). *Net Present Value (NPV): What it Means and Steps to Calculate it*. [Online]. Available: <https://www.investopedia.com/terms/n/npv.asp>
- [31] F. Fan, G. Zorzi, D. Campos-Gaona, and J. Nwobu, "Wind-plus-battery system optimisation for frequency response service: The U.K. perspective," *Electr. Power Syst. Res.*, vol. 211, Oct. 2022, Art. no. 108400, doi: [10.1016/j.epsr.2022.108400](https://doi.org/10.1016/j.epsr.2022.108400).
- [32] P. Mercier, R. Cherkaoui, and A. Oudalov, "Optimizing a battery energy storage system for frequency control application in an isolated power system," *IEEE Trans. Power Syst.*, vol. 24, no. 3, pp. 1469–1477, Aug. 2009.
- [33] W. Ou, R. Dunn, W. Kong, J. Yu, and Q. Li, "Optimal allocation of battery energy storage system in the U.K. power system for the frequency regulation with high wind penetration," in *Proc. IEEE/IAS Ind. Commercial Power Syst. Asia (I CPS Asia)*, Jul. 2020, pp. 1192–1197.

...